

EFFECT OF SHEAR ON DROPLETS IN A BINARY MIXTURE

ALEXANDER J. WAGNER

and

J. M. YEOMANS

*Theoretical Physics, University of Oxford, 1 Keble Rd.
Oxford OX1 3NP, United Kingdom*

Received (May 16, 2018)

Revised (revised date)

In this article we use a lattice-Boltzmann simulation to examine the effects of shear flow on an equilibrium droplet in a phase separated binary mixture. We find that large drops break up as the shear is increased but small drops dissolve. We also show how the tip-streaming, observed for deformed drops, leads to a state of dynamic equilibrium.

1. Introduction

The study of phase transitions under shear has been of great interest in the recent past^{1,2,3,4}. To understand the basic phenomena underlying this complex process we focus our attention on the behavior of a single equilibrium droplet in a two-dimensional binary fluid under shear flow. Despite the simplicity of the model system it shows rich behavior, both droplet break-up and droplet dissolution. We also suggest a new explanation of tip streaming observed in our simulations.

Consider first an immiscible drop subjected to a shear flow. This problem has been studied extensively since the original experiments by Taylor⁵. Experimental, theoretical and numerical results are available in three dimensions^{6,7,8} and theoretical^{9,10} and numerical^{11,12} results in two dimensions. These approaches consider drops with a singular interface and a conserved volume. The drops are deformed by the shear flow while maintaining their volume. If the shear rate exceeds a certain critical value, which depends on the volume of the drop, the drop will break up. Conversely, for a given shear rate, there exists a volume above which the drop is unstable. We shall denote this volume V_b .

For a miscible binary mixture a similar break-up of droplets is observed if the droplets are large. However there is now a second volume scale V_d which sets a *lower* limit to the drop size. V_d corresponds to the minimum size of a nucleation seed. The reason for the existence of V_d lies in the free energy balance between the favorable creation of separate phases in the supersaturated mixture and the unfavorable creation of the interface separating them. Note that, because when a

shear is applied a drop deforms and increases its surface length, V_d will depend on the shear rate. For shear rates with $V_b < V_d$ there are no stable drops in the system.

To study these phenomena we use a model developed by Orlandini *et.al.*¹³ for the isothermal flow of a binary mixture. In this approach a free energy which describes a binary fluid is chosen. The pressure tensor and chemical potential calculated from this free energy are then included in a lattice Boltzmann scheme for modeling fluid flow. The fluid obeys the Navier-Stokes and convection-diffusion equations and comes to an equilibrium corresponding to the minimum of the input free energy. The coexistence curve is correct and interfaces are extended in space as predicted by the Cahn-Hilliard theory. One advantage of this approach is that the free energy and the chemical potential can easily be calculated as local functions and compared to theoretical predictions.

In the next section of the paper we outline the thermodynamics of the binary fluid and describe the extensions to the lattice Boltzmann approach needed to treat shear flow. Results for the break-up of a large droplet are presented in section three. In section four we obtain an estimate for the volume V_d below which small droplets dissolve and discuss the effect of shear flow on the dissolution. Section five discusses tip streaming, the loss of material from the tips of the deformed droplet, and summarizes the results of the paper.

2. Method

We simulate a binary fluid comprising two components A and B, say. A–A and B–B interactions are zero but there is an A–B repulsion $\lambda n_A n_B$ where n_A and n_B are the number densities of A- and B-particles respectively. This system can be described by the Landau free energy functional

$$\Psi = \int d\mathbf{r} (\psi(\varphi, n, T) + \frac{\kappa}{2} (\nabla\varphi)^2) \quad (1)$$

where T is the temperature, $n = n_A + n_B$, $\varphi = n_A - n_B$ and κ is a measure for the interface free energy (surface tension). The free energy density of the homogeneous system is

$$\begin{aligned} \psi(\varphi, n, T) = & \frac{\lambda n}{4} \left(1 - \frac{\varphi^2}{n^2} \right) - Tn \\ & + \frac{T}{2} (n + \varphi) \ln \left(\frac{n + \varphi}{2} \right) + \frac{T}{2} (n - \varphi) \ln \left(\frac{n - \varphi}{2} \right). \end{aligned} \quad (2)$$

The Navier-Stokes and convection-diffusion equations for the fluid are simulated using a lattice Boltzmann approach described in detail in ^{13,14}. Here we restrict ourselves to a description of the way in which shear flow was implemented.

We consider a linear shear flow with velocity

$$\begin{pmatrix} u_x \\ u_y \end{pmatrix} = \begin{pmatrix} Gy \\ 0 \end{pmatrix} \quad (3)$$

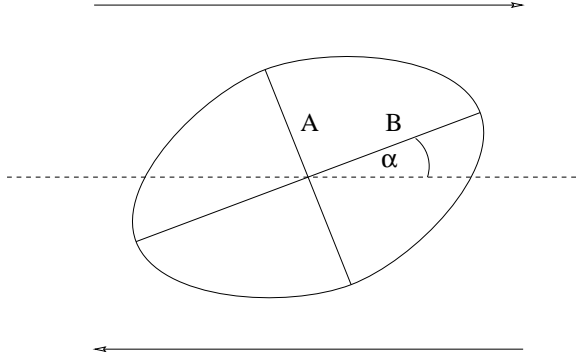


Figure 1: Sketch of a deformed drop in a simple shear flow. For small shear rates the drop has the form of an ellipse with axes $2A$ and $2B$. The ellipse is inclined to the direction of the shear flow by a shear strength dependent angle α .

where G is the shear rate. If the fluid is homogeneous it is expected that eqn.(3) describes the velocity field of the whole fluid. Inserting a droplet will disturb the velocity field locally but eqn.(3) gives the far field solution.

To simulate the shear it is necessary to introduce boundary conditions that force the flow. After each streaming step we replace the collision step at the boundary by a step that defines the variables of the lattice Boltzmann scheme to take values that correspond to the required value of the velocity and densities.

Two different kinds of boundary conditions have been implemented:

periodic: The top and bottom edges of the lattice at $y = \pm y_b$ are the boundaries and the velocity is constrained to be $\mathbf{u} = (Gy, 0)$. The side boundaries have periodic boundary conditions. This corresponds to a shear confined by two moving walls acting on a periodic array of drops.

forced: All the edges of the lattice are forced to have $\mathbf{u} = (Gy, 0)$. This eliminates the effects of periodic images of the drop. The local values of n and φ are replaced by their mean value averaged over the boundary. These boundary conditions generalize for more complicated forced flows, for example hyperbolic shear flow.

For a homogeneous system both boundary conditions lead to the velocity profile of eqn.(3) to within machine accuracy. In the presence of a drop both boundary conditions are expected to give the same results for an infinite lattice. A comparison of the two different boundary conditions therefore gives a measure of the effect of the periodic images on the drop.

If a drop is placed in a shear flow it will be deformed by the forces acting on it. The drop elongates and turns to lie at an angle α to the flow until in the steady state the restoring force due to the surface tension balances the shear forces acting upon the drop. This situation is sketched in figure 1. For small deformations the

4 Effect of shear on droplets in a binary mixture

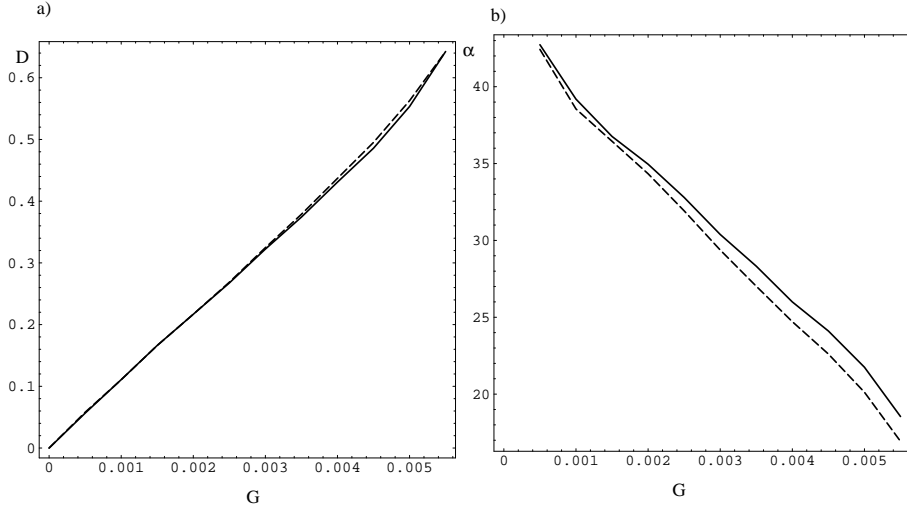


Figure 2: a) Deformation of a drop D and b) the tilting angle α for periodic (—) and forced (- - -) boundary conditions against the shear rate G . The undeformed drop has a radius of 8 lattice spacings and the lattice size is 60x30.

drop approximates well to an ellipse and its deformation can be defined as

$$D = \frac{A - B}{A + B} \quad (4)$$

where A and B are the major and minor axes respectively. For drops of constant volume the deformation and inclination angle depend only on a dimensionless quantity, the capillary number⁶

$$Ca = \frac{\nu a G}{\sigma} \quad (5)$$

where ν is the viscosity, a the undeformed drop radius and σ the surface tension. Throughout this paper we take $\nu = 1/6$ and $\sigma = 0.046$ ($\kappa = 0.002$). This corresponds to an interface width ≈ 3 lattice spacings.

3. Break-up

Typical results for large drops ($V \gg V_d$) are shown in figure 2 where D and α are plotted as function of the shear rate. Results for forced and periodic boundary conditions are compared. The results presented are for a lattice of size 60x30 with a drop of initial radius 8. They were obtained by equilibrating the fluid at each data point and then increasing the shear, re-equilibrating to give the next point, and so on.

There is a linear dependence of the deformation on the shear rate for small shear rates, followed by a more rapid deformation as the shear increases, and finally break up. The different boundary conditions lead only to small quantitative differences in

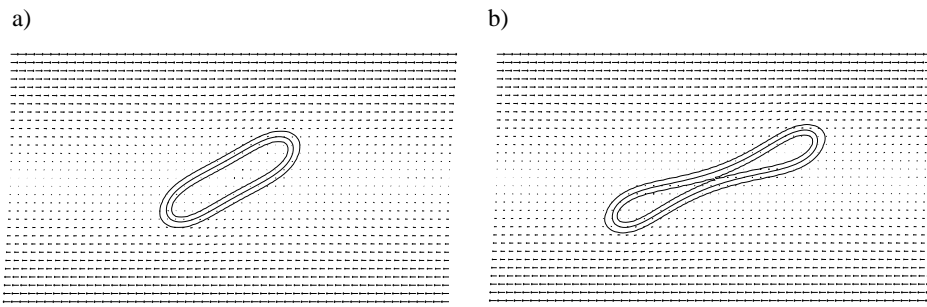


Figure 3: a) An equilibrium drop at $G = 0.002246$, b) the same drop at $G = 0.002251$ in the first stage of breaking up. The drop in b) breaks up into two drops of equal size at larger times. The arrows show the velocity at every third lattice point in each direction.

the result. The results are in qualitative agreement with the results expected from comparison with three-dimensional experiments. For a drop of constant volume and given ratio of the viscosity of the drop and the surrounding fluid the deformation depends only on the capillary number⁶. The drops studied here do not have a constant volume and therefore deformation at break up should depend on the parameters of the system but it is reasonable to expect only a weak dependence. Indeed we find $D_b \approx 0.65$ for drops with undeformed radii 8,13,20 in those cases where they break up.

It is known⁷ that the second curvature is very important for the rupture of three-dimensional drops. This mechanism does not exist in two-dimensional systems. Therefore we felt it was important to check the existence of the break up carefully, particularly as it is well known⁷ that a sudden change in shear strength can lead to rupture long before the critical shear rate. We therefore performed careful numerical simulations where we saved a stationary solution and then increased the shear flow. If the drop ruptured instead of reaching a stationary state we loaded the old configuration and increased the shear rate by only half the previous amount. We iterated this step until the increase in shear rate was smaller than a lower bound. The shear rate never grew larger than a previously rejected shear rate showing that the break-up is not due to non-equilibrium effects. We then decreased the shear rate to check that the system is in equilibrium at every point. No hysteresis effects were observed showing that this is indeed the case.

It should be pointed out, however, that the rupture mechanism is very different in two and three dimensions. Three dimensional drops break up into two main drops and satellite drops⁷. We observe that two dimensional drops break up into two drops of equal size as shown in figure 3.

4. Dissolution

For given n_A , n_B , T , if a binary fluid lies in the coexistence region it will separate

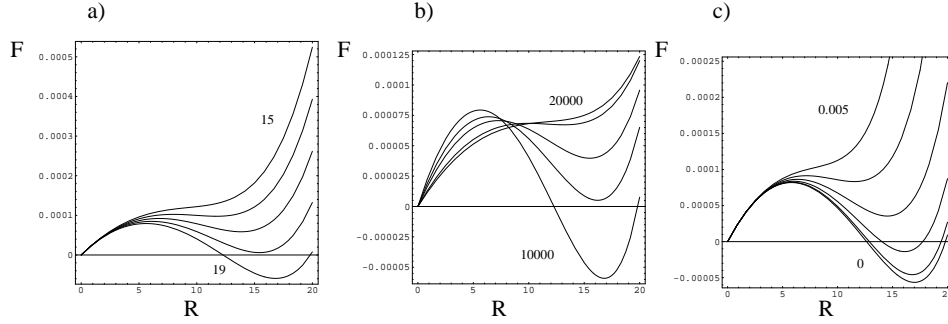


Figure 4: The free energy plotted as function of the drop radius for a) a lattice with 10000 points for concentrations that without surface effects would correspond to drops of radii $R^0 = 15, 16, 17, 18$ and 19 ; b) a system with $R^0 = 19$ and lattice sizes 10000, 12000, 14000, 16000, 18000 and 20000; c) a system of size 10000 and $R^0 = 19$ for shear rates $G = 0, 0.001, 0.002, 0.003, 0.004$ and 0.005 .

into two phases with concentration differences φ_1 and φ_2 , say. Each phase occupies a fraction of the total volume of the system which is determined by the densities and temperature. For a finite system the interface between the two phases results in a finite positive contribution to the free energy and, if this is too large relative to the gain in free energy due to the phase separation, the drop is unstable.

For the model simulated here it is possible to obtain an estimate of the droplet volume below which dissolution will occur. Ignoring the interface curvature the surface tension for an interface orthogonal to the z -direction is¹⁵

$$\sigma = \kappa \int_{-\infty}^{\infty} \left(\frac{\partial \varphi}{\partial z} \right)^2. \quad (6)$$

Hence, using (1) the free energy of a drop of radius R in a volume V is

$$F = \pi R^2 \psi(\varphi_1, n, T) + (V - \pi R^2) \psi(\varphi_2, n, T) + 2\pi R \sigma. \quad (7)$$

This should be minimized with respect to R , φ_1 and φ_2 where one variable can be eliminated by the constraint

$$\pi R^2 \varphi_1 + (V - \pi R^2) \varphi_2 = \varphi. \quad (8)$$

In figure 4a the free energy, relative to that of a homogeneous system, is plotted as a function of the drop radius for different concentrations of A and B particles. The concentrations are chosen such that without the surface effects drops of radii 15, 16, 17, 18, and 19 would minimize the free energy on a lattice of size 100x100. We will denote these radii by R^0 . Without the surface free energy term there is only one minimum and this will always be reached. With surface effects the homogeneous phase ($R = 0$) is always stable and a finite deviation from it is needed to reach the

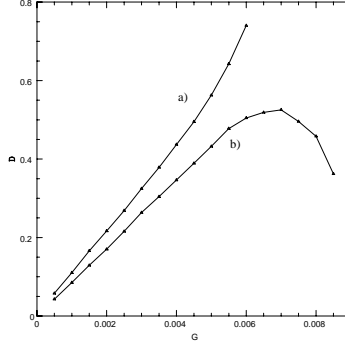


Figure 5: Deformation as function of shear rate for a drop of radius 8 for systems of size a) 60x30, b) 70x40. The drop in the smaller system breaks up while the drop in the larger system dissolves. Because the mass of the drop decreases strongly at high shear rates its deformation decreases under the increase of shear before it completely dissolves.

global minimum. This corresponds to the metastability of some regions of phase space where a finite nucleation barrier prevents immediate phase separation.

The lowest free energy curve in figure 4a corresponds to $R^0 = 19$. The figure shows that the effect of the surface free energy is to shift the minimum from 19 to about 16.7. For smaller R^0 the minimum becomes a local minimum at $R^0 \approx 18$. In systems with fluctuations this will eventually lead to the drops dissolving. However the lattice Boltzmann simulations reported here do not include noise and a drop in a local minimum will be stable. For concentration ratios that lead to a graph that has no local minimum ($R^0 \gtrsim 15.5$) the drop will dissolve. However we observe that the initial dynamics are very slow.

The radius below which drops dissolve depends not only on the size of the drop but also on the total volume of the system. Results for the concentration corresponding to $R^0 = 19$ for different system sizes are shown in figure 4b. Droplets are less stable in a larger system because more material from the drop is needed to change the concentration outside the drop.

When shear is applied the droplets deform. They have a larger interface so that the surface contributions are increased. For small shear rates the dependence of the deformation on the shear rate is approximately linear and we can use

$$D \approx 10GR \quad (9)$$

where R is the radius of the undeformed drop with the same volume. Approximating the shape of the deformed drop by an ellipse the length of the interface is given by

$$L = \sqrt{\frac{1-D}{1+D}} E \left(-\frac{4D}{(1-D)^2} \right) \quad (10)$$

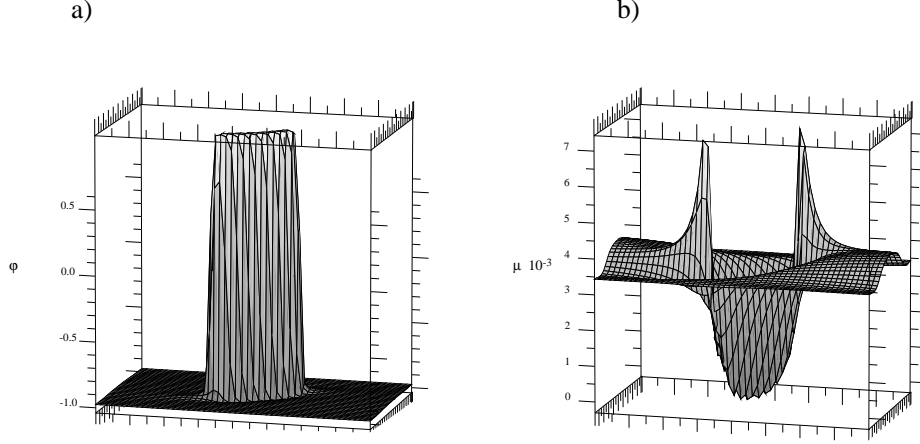


Figure 6: a) The density difference φ and b) the chemical potential μ for a highly deformed drop.

where $E(k)$ denotes the complete elliptic integral of the second kind. This result can be used to estimate the effect of shear flow on the free energy. The results for $R^0 = 19$ for different shear rates are shown in figure 4c. The minimum in the free energy vanishes for high shear rates and no stable drops can exist. This corresponds to the dissolution of a drop under shear.

The effects predicted by the thermodynamic theory are observed in the simulations. In figure 5 results for the simulation of a drop of $R^0 = 8$ on lattices of size 60×30 and 70×20 are shown. For the smaller lattice $V_b < V_d$ and the drop breaks up. For the larger lattice the drop can exist to larger values of the shear, but loses mass. Finally as the shear is increased further it dissolves.

It is interesting to note that the theory predicts that every drop will dissolve under shear in a sufficiently large system. That is because the mass loss from the drop has to change the concentration outside the drop in order to reach a new equilibrium. This can, however, be very difficult to observe because there is a separation of time scales. The time t_D needed for diffusion to equilibrate the system scales as $t_D \sim L^2$ where L is the length of the system. This result is altered under shear¹⁶ and in the limit of very large shear rates $t_D \sim L^{\frac{3}{2}}$. The time t_F for the system to reach a steady flow and a new deformation of the bubble scales as $t_F \sim L$. Therefore in large systems the time for the deformation of the drop will be fast compared to the time for it to dissolve.

5. Discussion

In our previous discussion we have assumed that thermodynamic arguments for equilibrium can be carried over to the stationary states of dynamic systems. This is, however, not necessarily the case. We observe a deviation from this assumption in a phenomenon which we will call “tip-streaming”. Mass is pulled from the ends of the drop by the shear flow. The depletion of the concentration in the drop leads to a reduction of the chemical potential in the drop. The non-constant chemical potential leads to a diffusion current acting in the direction of the chemical potential gradient which returns material to the drop. Equilibrium is reached when the diffusion into the drop balances the tip streaming. The chemical potential in dynamic equilibrium is shown in fig.6b. Note that this is a state of dynamic equilibrium not thermodynamic equilibrium as μ is not constant.

For a small diffusion constant a large chemical potential difference is needed for equilibrium and hence a large amount of mass is pulled from the drop. This mechanism for the dissolving of a drop is distinct from the free energy driven mechanisms explained earlier in the paper. It depends on the diffusion constant which is a dynamical quantity that does not enter the free energy. For infinite diffusion, however, material is immediately returned to the drop and no difference in the chemical potential is set up. A similar tip-streaming was observed in experiments but was interpreted as a surfactant effect ⁷.

Halliday *et.al.* performed simulations on a droplet in a binary fluid using a derivative of the the Gunstensen¹⁷ algorithm. They obtain a similar break-up behavior but there are some important differences in the results. In particular in the simulations reported here all equilibrium drops are convex (see figure 3) whereas Halliday *et.al.*¹² report stationary drops that are constricted in the middle. They also observe smaller inclination angles α at break up. The discrepancies warrant further investigation. Another feature not reported by Halliday *et.al.* is the dissolution of drops under shear. This may be due the fact that they work in a region where the two components are more strongly separated. Nevertheless small droplets should still dissolve. We caution that the time-scale for dissolution can be much larger than that for the deformation of the droplet to reach an equilibrium value.

Goldburg and Min³ performed experiments on nucleation in a binary mixture in the presence of shear. They observed the vanishing of drops under the influence of shear as a sharp transition. This transition may be interpreted as corresponding to the point where $V_b = V_d$.

To conclude, in this paper we have shown that drops under increasing shear flow can either break up or dissolve. We explained this behavior with thermodynamic arguments. Tip-streaming was shown to lead to a state of dynamic equilibrium for deformed droplets.

Acknowledgments

We thank E. Orlandini, C. Care, and I. Halliday for helpful discussions. A.J.W. thanks J. Schlosser for providing visualization software. J.M.Y. acknowledges support from the EPSRC, UK and NATO.

References

1. J.F. Olson and D.H. Rothman, *J. Stat. Phys.* **81**: 199-222 (1995).
2. D. Jasnov and J. Vinals *J. Fluids* **8**: 660-669 (1996)
3. W.I. Goldburg and K.Y. Min, *Physica A* **204**: 246-260 (1994)
4. J. Lauger, C. Laubner, and W. Gronski *Phys. Rev. Lett.* **75**: 3576-3579 (1995).
5. Taylor, G.I., *Proc. Roy. Soc.* **26**: 501-523 (1934).
6. Rallison, J.M., *Annu. Rev. Fluid Mech.* **16**: 45-66 (1984).
7. Stone, H.A., *Annu. Rev. Fluid Mech.* **26**: 65-102 (1994).
8. Rallison, J.M., *J. Fluid Mech.* **109**: 465-482 (1981).
9. Richardson, S., *J. Fluid Mech.* **33**: 476-493 (1968).
10. J.D. Buckmaster and J.E. Flaherty, *J. Fluid Mechanics*, **60**: 625-639 (1973).
11. I. Halliday and C.M. Care, *Phys. Rev. E* **53**: 1602-1612 (1996)
12. I. Halliday, C.M. Care, S. Thompson, and D. White, *Phys. Rev. E* **54**: 2573-2576 (1996).
13. E. Orlandini, M.R. Swift, and J.M. Yeomans, *Europhys. Lett.* **32**: 463-468 (1995).
14. M.R. Swift, E. Orlandini, W.R. Osborn, and Yeomans, J.M., *To be published in Phys. Rev. E*.
15. J.S. Rowlinson and B. Widom, *Molecular theory of capillarity*, Clarendon Press, Oxford (1982).
16. M.J. Howard and G.T. Barkema, *Phys. Rev. E* **53**: 5349-5956 (1996).
17. A.K. Gunstensen, D.H. Rothmann, S. Zaleski, and G. Zanetti, *Phys. Rev. A* **43**, 4320 (1991)